STRESS DISTRIBUTION ANALYSIS ON ADHESIVELY BONDED SINGLE LAP JOINT USING EXPERIMENTAL OPTICAL METHOD

M.H.F. Cunha, marcospinheiral@yahoo.com.br
L.F. Garcia Jr., luiznirvaneiro@yahoo.com.br
L.C.S. Nunes, luizcn@mec.uff.br

Universidade Federal Fluminense - UFF
Departamento de Engenharia Mecânica - TEM
Pós-Graduação em Engenharia Mecânica - PGMEC
Laboratório de Mecânica Teórica e Aplicada - LMTA
Rua Passo da Pátria, 156, Bloco E, Sala 216, Niterói, RJ CEP 24210-240, Tel.: 2629-5588

Abstract. *This paper presents an investigation relating to stress distribution in single lap joints. Two-dimensional experimental analyses are conducted via Digital Image Correlation-DIC method. This method is an optical-numerical experimental approach developed for full-field and non-contact measurements of surface displacement and deformation. Experimental results are compared with mechanics model for adhesively bonded lap joints, considering only linear elastic analyses. In this process, classical theoretical predications proposed by Goland & Reissner and Hart & Smith are used. In order to validate the experimental and analytical results, a commercially available finite element code is also used. The principal main is to use experimental approach to improve the mechanical performance and a better understanding of the mechanics of adhesive joints.*

Keywords*: Stress analysis, Single lap joint, Digital Image Correlation method*

1. INTRODUCTION

The use of adhesive joints have recently been increasing due to their improved mechanical performance and provides a better understanding of mechanical behaviour of structure commonly found in aerospace, marine and automotive industries. Because of this, a lot of works has been done on stress analysis and modeling of adhesively bonded single-lap joint under tension (Neves *et al.,* 2009, Silva *et al.,* 2009).

The first model, proposed by Volkersen in 1938 (Dillard and Pocius, 2002), is one of the most fundamental concepts in the transfer of load between two members joined by an adhesive. In 1944, Goland and Reissner developed a model considering the effects of the adherend bending and the peel stress, as well as the shear stress, in the adhesive layer in a single lap joint. This paper has been widely employed in the adhesive stress analysis and it is considered as a classical model which all recent works take it as reference. In 1973 Hart-Smith improved the Goland and Reissner adding the plasticity effects and Tsai *et al.* (1998) propose an alternative form. Recently, Luo and Tong (2009) developed a novel closed-form and accurate nonlinear solutions for single lap adhesive bonded joints. Practically, all works present theoretical and numerical analyses, but rarely one experimental analysis (Cognard *et al.* 2008, Tsai and Morton , 1995, Wang *et al.*, 2008).

The aim of this work is to use an experimental method, know as Digital Image Correlation (DIC), to analyze the displacement, strain and stress at the single lap joint. The DIC is a non-contact optical technique that allows the full-field estimation of strains on a surface under an applied strength. Two works developed by Nunes *et al*. (2007 and 2008), takes into account the DIC method to analyze single lap joints. The experimental results are to compared and validate with analytical models.

2. LINEAR ANALYTICAL MODEL AVAILABLE IN THE LITERATURE

The first analysis proposed by Volkersen, was based on a simple shear lag model for load transfer from one adherend to another by a simple shearing mechanism alone. This model does not reflect the effect of the adherend bending and shear deformations. Goland and Reissner (1944) considered that the eccentric load path of single lap joint causes a bending moment besides a transverse force. Later, Hart-Smith (1973) presented an alternative formulation to treat single lap joints. The typical geometrical schema and material parameters for balanced single lap joints are illustrated in Fig 1.

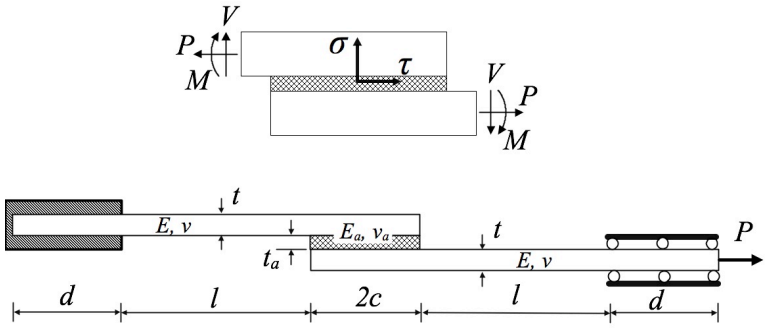

Figure 1. Typical geometrical schema of single-lap joint.

In Figure 1 the length of the overlap is 2*c*. The thickness of the outer and inner adherends is equal to *t*. *E* and ν are the Young's modulus and Poisson's ratio for the adherends, and E_a, ν_a and t_a are the corresponding adhesive Young's modulus, Poisson's ratio and thickness respectively. *P* is the applied force. The joint width is *b*.

2.1. Goland and Reissner's analysis

According of formulation presented by Goland and Reissner the distributions of the shearing at stress are expressed by the following equation

$$\tau = -\frac{1}{8}\frac{P}{bc}\left\{\frac{\beta c}{t}\left(1+3k\right)\frac{\cosh\left(\left(\beta c/t\right)\left(x/c\right)\right)}{\sinh\left(\beta c/t\right)}+3\left(1-k\right)\right\} \tag{1}$$

where the parameter β is defined as $\beta = \sqrt{8\frac{G_a}{E}\frac{t}{t_a}}$ and the bending moment factor is given by

$k = \dfrac{\cosh\left(u_2 c\right)}{\cosh\left(u_2 c\right)+2\sqrt{2}\sinh\left(u_2 c\right)}$ and the horizontal displacement is

$$u_2 = \sqrt{\frac{3\left(1-\nu^2\right)}{2}}\frac{1}{t}\sqrt{\frac{P}{btE}}$$

The distributions of the normal stress is given by

$$\sigma = \frac{1}{\Delta}\frac{Pt}{bc^2}\left[\left(R_2\lambda^2\frac{k}{2}+\lambda k'\cosh\left(\lambda\right)\cos\left(\lambda\right)\right)\cosh\left(\frac{\lambda x}{c}\right)\cos\left(\frac{\lambda x}{c}\right)+\left(R_1\lambda^2\frac{k}{2}+\lambda k'\sinh\left(\lambda\right)\sin\left(\lambda\right)\right)\sinh\left(\frac{\lambda x}{c}\right)\sin\left(\frac{\lambda x}{c}\right)\right] \tag{2}$$

where $\gamma^4 = 6\dfrac{E_a}{E}\dfrac{t}{t_a}$, $\lambda = \gamma\dfrac{c}{t}$, $k' = \dfrac{kc}{t}\sqrt{3\left(1-\nu^2\right)\dfrac{P}{btE}}$

$R_1 = \cosh\left(\lambda\right)\sin\left(\lambda\right)+\sinh\left(\lambda\right)\cos\left(\lambda\right)$ and $R_2 = \sinh\left(\lambda\right)\cos\left(\lambda\right)-\cosh\left(\lambda\right)\sin\left(\lambda\right)$

with $\Delta = \dfrac{1}{2}\left(\sin\left(2\lambda\right)+\sinh\left(2\lambda\right)\right)$

2.2. Hart-Smith's analysis

Taking the purely-elastic analysis developed by Hart-Smith which is a considerable improvement over the classical solution by Goland and Reissner, the distributions of the shear stress can be expressed by

$$\tau = A_2\cosh\left(2\lambda' x\right)+C_2 \tag{3}$$

where the parameter is defined by $\lambda' = \sqrt{\frac{\left[1+3\left(1-\nu^2\right)\right]}{2}\frac{G_a}{t_a E t}}$ and constants are given by

$$A_2 = \frac{G_a}{t_a E t}\left[\frac{P}{b}+\frac{6\left(1-\nu^2\right)M}{t}\right]\frac{1}{2\lambda'\sinh\left(2\lambda' c\right)} \text{ and } C_2 = \frac{1}{2c}\left[\frac{P}{b}-2\frac{A_2}{2\lambda'}\sinh\left(2\lambda' c\right)\right]$$

the bending moment is

$$M = \frac{P}{b}\left(\frac{t+t_a}{2}\right)\frac{1}{1+\xi c+\left(\xi^2 c^2/6\right)} \text{ with } \xi = \sqrt{\frac{P}{bD}}$$

The distributions of the normal stress is given by

$$\sigma = A\cosh\left(\chi x\right)\cos\left(\chi x\right)+B\sinh\left(\chi x\right)\sin\left(\chi x\right) \tag{4}$$

where $\chi^4 = \frac{E_a}{2Dt_a}$ with $D = \frac{Et^3}{12\left(1-\nu^2\right)}$

and the constants is $A = -\frac{E_a M\left[\sin\left(\chi c\right)-\cos\left(\chi c\right)\right]}{t_a D\chi^2\exp\left(\chi c\right)}$ and $B = \frac{E_a M\left[\sin\left(\chi c\right)+\cos\left(\chi c\right)\right]}{t_a D\chi^2\exp\left(\chi c\right)}$

3. DIGITAL IMAGE CORRELATION (DIC) METHOD

Digital Image Correlation (DIC) is an optical-numerical full-field surface displacement measurement method (Dally and Riley, 2005). It is based on a comparison between two images of a specimen coated by a random speckled pattern in the undeformed and in the deformed states. Its special merits encompass non-contact measurements, simple optic setups, no special preparation of specimens and no special illumination.

The basic principle of the DIC method is to search for the maximum correlation between small zones (subsets) of the specimen in the undeformed and deformed states, as illustrated in Fig. 2. From a given image-matching rule, the displacement field at different positions in the analysis region can be computed. The simplest image-matching procedure is the cross-correlation, which provides the in-plane displacement fields $u(x,y)$ and $v(x,y)$ by matching different zones of the two images.

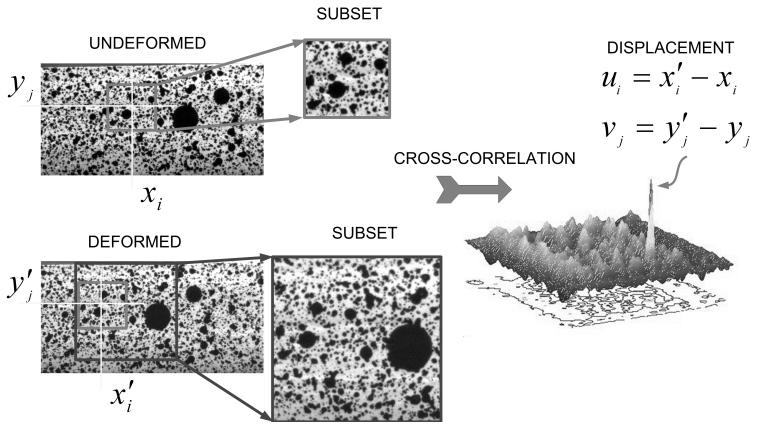

Figure 2. Schematic of the principle of digital image correlation

A commonly used correlation coefficient is defined as follows

$$c(u,v)=\frac{\sum_{i=1}^{m}\sum_{j=1}^{n}\left[f\left(x_i,y_j\right)-\bar{f}\right]\left[g\left(x'_i,y'_j\right)-\bar{g}\right]}{\sqrt{\sum_{i=1}^{m}\sum_{j=1}^{n}\left[f\left(x_i,y_j\right)-\bar{f}\right]^2}\sqrt{\sum_{i=1}^{m}\sum_{j=1}^{n}\left[g\left(x'_i,y'_j\right)-\bar{g}\right]^2}} \tag{5}$$

$$\begin{aligned} x' &= x+u_0+\frac{\partial u}{\partial x}dx+\frac{\partial u}{\partial y}dy \\ y' &= y+v_0+\frac{\partial v}{\partial x}dx+\frac{\partial v}{\partial y}dy \end{aligned} \tag{6}$$

where $f\left(x,y\right)$ is the pixel gray level value (ranging from 0 to 255) at the coordinates $\left(x,y\right)$, for the undeformed or original image; $g\left(x',y'\right)$, is the pixel gray level value at the coordinates $\left(x',y'\right)$ for the deformed or target image; $\bar{f}$ and $\bar{g}$ are the average gray values for images and, finally, u and v are, respectively, the displacement components for the subset centers in the x and y directions.

4. RESULTS AND DISCUSSION

4.1. Numerical results

In this section, it will be presented numerical results obtained using a commercially available finite element code. The numerical results are also compared with those predicted by Goland and Reissner and Hart-Smith models according with Eqs. (1) and (3), respectively. In Figure 3, the adhesive shear stress distribution for aluminum alloy adherends and epoxy adhesive is presented. In this analysis, it was taken into accounting for adherends and adhesive the following geometry and mechanical parameters: length of the overlap, 2c = 28 mm; the thickness of the outer and inner adherends, t = 1.6 mm; the Young's modulus E = 69 GPa and Poisson's ratio ν = 0.33 for the adherends and E_a =2.4 GPa, ν_a =0.35 and t_a =0.3 mm are the corresponding adhesive Young's modulus, Poisson's ratio and thickness respectively. The applied force P = 1.5 kN.

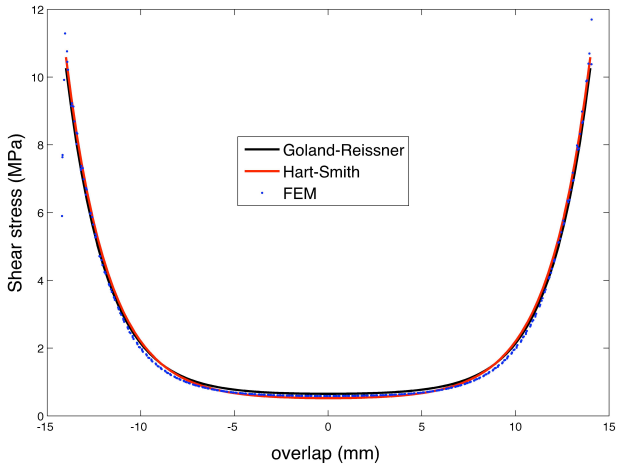

Figure 3. The adhesive shear stress distribution

Figure 3 shows good agreement between Goland and Reissner, Hart-Smith modes and FE method. This analysis was made to make sure the results.

4.2. Experimental results

The experimental arrangement involves an apparatus developed to apply strain in a single lap joint, a CCD camera set perpendicularly to the specimen and a computer to capture and process the images, as shown in Fig. 4. The single lap joint, fixed in the strain apparatus in agreement with the geometrical model as shown in Fig. 1, was covered with painted speckles (random black and white pattern). Two images of this single lap joint were recorded using the CCD

camera, before and after load, with a resolution of 1392x1040 pixels. In this experimental configuration one pixel of the CCD camera corresponds to an area of about 4.63×4.63 μm on the object.

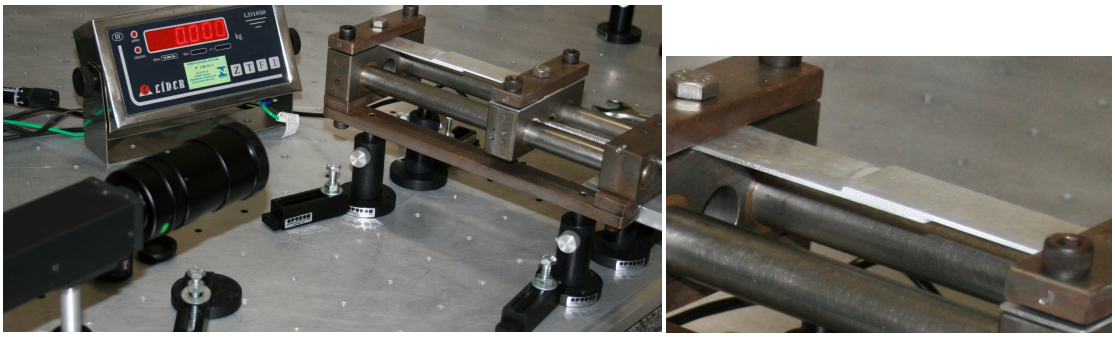

Figure 4. Experimental arrangement with strain apparatus of bonded joint details.

In order to obtain the experimental results, the geometry model for the single lap joint, schematically illustrated in Fig. 1, was considered with the following data: (a) Applied force, P = 1.5 kN; (b) length of restraint against transversal motion, d = 25.4 mm; segment of length, l = 49.6 mm; joint length, $2c$ = 28 mm; adherend and adhesive thickness, t = 1.6 mm and t_a = 0.3 mm, respectively. The upper and lower adherends have the same characteristics and the material proprieties of adherends and adhesive are shown in Tab.1.

Table1. Material Proprieties of adherend and adhesive.

	Material	Young's Modulus, E (GPa)	Poisson's ratio, ν
Adherend	Aluminum alloy	69	0.33
Adhesive	Epoxy adhesive	2.4	0.35

In this analysis, it is take into account only a half of overlap because of symmetry presented in Fig 3. The two images of the single lap joint cover with painted speckles are taken in the same region, as illustrated in Figure 5, considering two different loads of 0 and 1.5k N. These images were used to determinate full-field displacement by means of computer software based on correlation theory, presented in item 3.

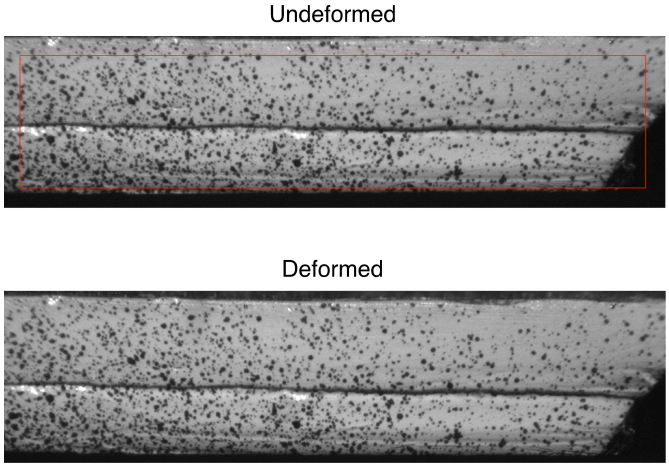

Figure 5. Pattern of coating specimen underformed and deformed.

The results of the full-field displacement $u(x,y)$ and $v(x,y)$, associated with x and y directions respectively, are shown in Fig. 6. These results are obtained inputting the underformed and the deformed images for different loads of 0 and 1.5 kN into DIC program.

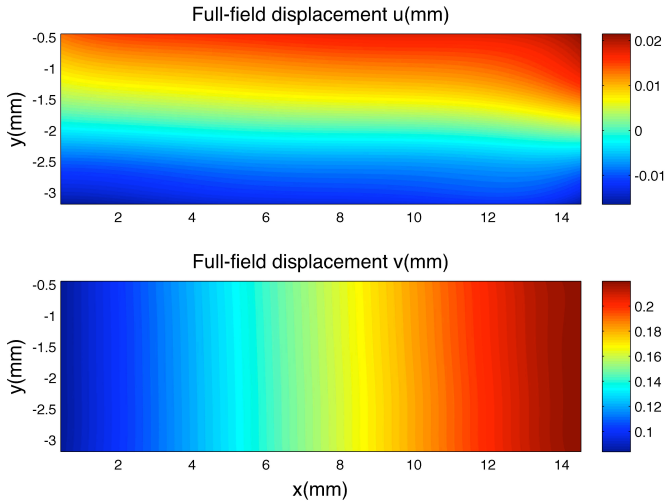

Figure 6. Experimental results: $u(x,y)$ is the horizontal full-field displacement and $v(x,y)$ is the vertical full-field displacement.

Taking the results of full-field displacements $u(x,y)$ and $v(x,y)$, it can be obtained some important information like the normal strain in both directions, i.e., ε_x and ε_y, and the shear strain ε_{xy}. These results are illustrated in Fig. 7.

Here the principal objective is to analyze the shear stress. For this, let us consider the particular case of the shear strain ε_{xy}. It may be seen in Fig 7 that the distortion of outer and inner adherends is the approximately constant. However, the distribution of shear strain at adhesive varies as a function of x, increasing at end of overlap.

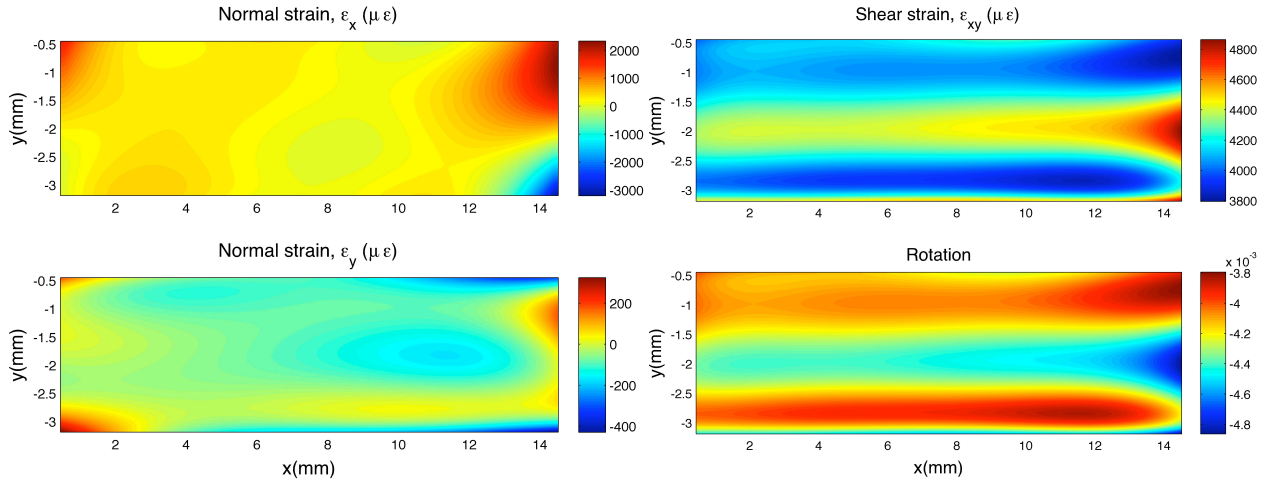

Figure 7. Full-field distribution around the half overlap: normal and shear strain; rotation

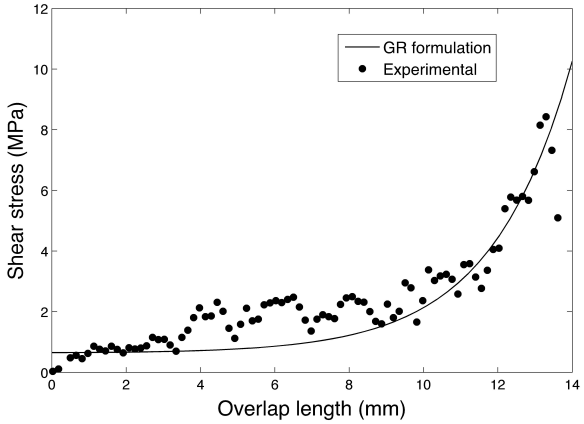

Figure 8. The adhesive shear stress distribution versus half length of overlap. Comparison between Goland-Reissner formulation and experimental results.

In order to validate the experimental results, the distribution of shear stress at middle of overlap, i.e., $y = 0$, is taken and it is compared with Goland and Reissner formulation previously presented in Eq (1). It is important note that to obtain the shear stress is necessary to multiply the shear strain by the adhesive shear modulus, because it is assumed an elastic behaviour.

Figure 8 shows a good agreement between the distribution of shear stress obtained experimentally and the classical formulation developed by Goland and Reissner. It can be observed that the maximum value of shear stress occurs at overlap end, approximately equal to 8.4 MPa.

5. CONCLUTIONS

This work aimed at using experimental information obtained from Digital Image Correlation method to analyze single lap joint. DIC method was used to obtain the displacement field of specific regions. The results indicate good agreement between experimental results and classical model.

The main contribution of this work is to provide an experimental method of estimating the full field displacement and shear stress in a single lap joint.

6. ACKNOWLEDGEMENTS

The authors would like to express their gratitude to the Ministry of Science and Technology. The present paper received financial support from Brazilian agencies CNPq and FAPERJ

7. REFERENCES

Dillard, D.A., Pocius, A.V., 2002, "Adhesion Science And Engineering – I" , The Mechanics Of Adhesion, Elsevier Science B.V., First Edition.

Cognard , J.Y., Créac'hcadec, R., Sohier, L., Davies, P., 2008, "Analysis of the nonlinear behavior of adhesives in bonded assemblies—Comparison of TAST and Arcan tests", International Journal of Adhesion & Adhesives, Vol. 28, pp. 393– 404.

Dally, J.W. and Riley, W.F., 2005 "Experimental Stress Analysis", 4 ed., McGraw Hill.

Goland, M., Reissner, E., 1944, "The stresses in cemented joints", Journal of Applied Mechanics, Vol 11, pp. A17–A27.

Hart-Smith, L.J., 1973, "Adhesive-bonded single-lap joints", NASA, CR-112236.

Luo, Q., Tong, L., 2009, "Analytical solutions for nonlinear analysis of composite single-lap adhesive joints", International Journal of Adhesion & Adhesives, Vol. 29, pp. 144– 154

Neves, P.J.C., Adams, R.D., Spelt, J.K., 2009, "Analytical models of adhesively bonded joints—Part I: Literature survey", International Journal of Adhesion & Adhesives, Vol 29, pp. 319–330.

Nunes, L.C.S., Dias, R.A.C., Nascimento, V.M.F., Santos, P.A.M., 2007, "Analysis of Adhesive Bonding using Digital Image Correlation Technique", In: Proceedings of the 19th International Congress of Mechanical Engineering, Brasília.

Nunes, L.C.S., Dias, R.A.C., Santos, P.A.M., 2008, "Análise Numérica, Analítica e Experimental do Comportamento Mecânico de Juntas Coladas", In: Proceedings of the V National Congress of Mechanical Engineering. Salvador.

Silva, L.F.M., Neves, P.J.C., Adams, R.D., Wang, A., Spelt, J.K., 2009, Analytical models of adhesively bonded joints-Part II: Comparative study, International Journal of Adhesion & Adhesives , Vol. 29, pp. 331–341.

Tsai, M.Y., Oplinger, D.W., Morton, J., 1998, "Improved Theoretical Solutions for Adhesive Lap Joints", International Journal of Solids and Structures, Vol 35, pp. 1163-1185.

Tsai, M.Y., Morton, J., 1995, "An experimental investigation of nonlinear deformations in single-lap joints", Mechanics of Materials, Vol. 20, pp. 183-194.

Wang, Z.Y., Wang, L., Guo, W., Deng, H., Tong, J.W., Aymerich , F., 2008, "An investigation on strain/stress distribution around the overlapend of laminated composite single-lap joints", Composite Structures, Vol., pp.

8. RESPONSIBILITY NOTICE

The authors are the only responsible for the printed material included in this paper.